PHYSICAL REVIEW E **81**, 065301(R) (2010)

Emergence of foams from the breakdown of the phase field crystal model

Nicholas Guttenberg,[1] Nigel Goldenfeld,[1] and Jonathan Dantzig[2]
[1]*Department of Physics, University of Illinois at Urbana-Champaign, 1110 West Green Street, Urbana, Illinois 61801-3080, USA*
[2]*Department of Mechanical Science and Engineering, University of Illinois at Urbana-Champaign, 1206 West Green Street, Urbana, Illinois 61801-3080, USA*
(Received 24 February 2010; published 9 June 2010)

The phase field crystal (PFC) model captures the elastic and topological properties of crystals with a single scalar field at small undercooling. At large undercooling, new foamlike behavior emerges. We characterize this foam phase of the PFC equation and propose a modified PFC equation that may be used for the simulation of foam dynamics. This minimal model reproduces von Neumann's rule for two-dimensional dry foams and Lifshitz-Slyozov coarsening for wet foams. We also measure the coordination number distribution and find that its second moment is larger than previously reported experimental and theoretical studies of soap froths, a finding that we attribute to the wetness of the foam increasing with time.

DOI: 10.1103/PhysRevE.81.065301 PACS number(s): 47.57.Bc, 64.70.D−, 47.54.−r

I. INTRODUCTION

Computational modeling of large-scale systems usually involves either detailed molecular-dynamics simulations, in which every particle must be tracked, or a highly coarse-grained model in which the underlying symmetries are known and are used to derive a continuum model from the underlying physics. Molecular dynamics is limited to small systems and/or to very short times, and coarse-grained models tend to fail at places where the underlying symmetries are broken, such as at defects and dislocations. The phase field crystal (PFC) model [1] is an intermediate approach with the advantage of diffusive time scale but with atomic scale resolution of molecular dynamics. The PFC model can be used to capture the dynamics of defects and dislocations in large crystals [2,3], the dynamics of grain interactions [4], molecular dynamics of vacancies [5], and even nonlinear elasticity [6]. In addition, it is amenable to methods such as coarse graining and adaptive mesh refinement [7].

The dimensionless phase field crystal equation [1],

$$\frac{\partial \psi}{\partial t} = \nabla^2[(\nabla^2+1)^2\psi + r\psi + \psi^3], \tag{1}$$

where ψ is a continuous density field and r is a parameter interpreted as an undercooling, is a density-functional theory [2], best thought of as arising from phenomenological and symmetry considerations. In particular, this is the simplest class of models appropriate for systems whose dynamics is governed by minimizing departures from periodicity [8], as opposed to the situation in other materials processes, such as spinodal decomposition, where the dynamics minimizes departures from spatial uniformity. In principle this approach only holds for small values of the undercooling r, beyond which the strong nonlinearity may in principle overwhelm the crystal's symmetries, leading to such artifacts as merger or dissolution of the "atoms" of the model.

In this Rapid Communication, we explore an interesting feature of the phase field crystal model in the limit of large undercooling, which we show turns out to facilitate a simple, scalar, and minimal model of foams. At large undercooling, the periodic phases found at low undercooling have higher free energy than a mixture of two immiscible liquids. The result is a coarsening foamlike structure, which we analyze in order to propose a minimal, modified PFC model that is capable of describing quantitatively both wet and dry foams at the level of a continuum scalar theory that is computationally efficient.

II. EQUILIBRIUM PHASE DIAGRAM

The phase diagram of the PFC model has been computed for small undercoolings [1]. We shall use the same methods to construct the phase diagram at larger values of the undercooling in order to see what may be found there. First, however, we will convert the PFC equation and PFC energy to a nondimensionalized form with respect to the equilibrium liquid (constant phase) density. We define a parameter related to the undercooling: $\alpha \equiv -r$. In terms of this new parameter, the energy minimizing density for the constant phase is $\psi = \pm\sqrt{\alpha}$, so we will introduce a nondimensional order parameter $\phi \equiv \psi/\sqrt{\alpha}$. This gives us the following free energy:

$$F = \int_V \frac{1}{2}\phi(\nabla^2+1)^2\phi + \alpha\left(-\frac{1}{2}\phi^2 + \frac{1}{4}\phi^4\right)dV \tag{2}$$

and corresponding equation of motion:

$$\frac{\partial \phi}{\partial t} = \nabla^2[(\nabla^2+1)^2\phi + \alpha(-\phi+\phi^3)]. \tag{3}$$

We then construct the phase diagram at large α by calculating the energy minima of the one-mode approximations for the constant phases $L_\pm: \phi = \phi_0$, where the subscript $\pm$ refers to the sign of the average density ϕ_0; the striped phase $S: \phi = \phi_0 + A_S\cos(x)$, where $A_S = \sqrt{\alpha(4-3\phi_0^2)/3}$; and the two triangular lattices $\Delta_\pm: \phi = \phi_0 + (A_\Delta \pm B_\Delta)[\cos(\vec{k}_1\cdot\vec{r}) + \cos(\vec{k}_2\cdot\vec{r}) + \cos(\vec{k}_3\cdot\vec{r})]$, where the $\vec{k}_j$ are the lattice vectors of the regular triangular lattice, $A_\Delta = -\alpha\phi_0/5$, and $B_\Delta = \sqrt{\alpha(15-36\phi_0^2)}/15$.

Even though the one-mode approximation is not accurate at these large values of α, we may use it to understand heuristically the behavior observed, thus motivating our form for

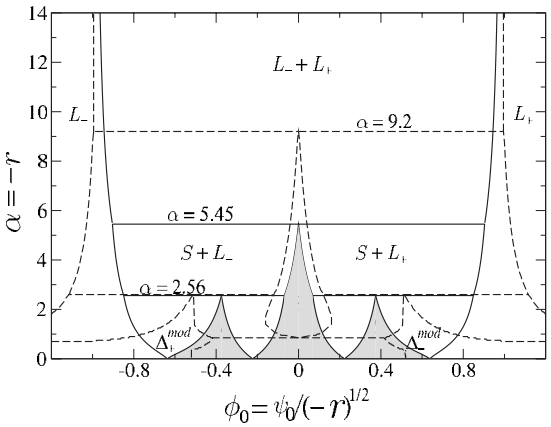

FIG. 1. Solid lines, phase diagram associated with the free energy in Eq. (2). Dashed lines, phase diagram associated with the modified free energy in Eq. (5).

the modified phase field crystal model introduced below. Our main results, for the modified phase field crystal model, are fully time-dependent and independent of this approximation.

The equilibrium phase diagram is obtained by substituting the various ansatz into Eq. (3) and performing a common tangent construction. The result is shown in Fig. 1 (solid lines). We find a series of previously undiscovered invariant points as α increases. At $\alpha=2.56$, the coexistence region between the striped and triangular phases disappears, giving rise to a coexistence between stripes and one of the liquid phases. Then, at $\alpha=5.45$ the striped phase vanishes, leaving only a region of immiscible liquid-liquid coexistence, and the regions comprised entirely of the liquid phases.

This can be understood by considering the influence of the two terms in the free energy. At small α, the wavelength selection term that was added to produce periodic phases is dominant. As α increases, the term that drives ϕ to have the values of ± 1 becomes dominant so that eventually the wavelength selection term $(1+\nabla^2)^2\phi$ is a small perturbation and the equilibrium phases are determined by the average value of $\phi_0^2/2-\phi_0^4/4$, which is minimized by the constant phases.

III. DYNAMICS

The phase diagram we have just computed represents the behavior of this system in its final equilibrium state. However, the approach toward that equilibrium changes as α increases. Starting from a hexagonal lattice, the system attempts to coarsen into two regions: one composed of L_+ and the other composed of L_-. However, because of the small residual wavelength selection, there is a finite energy cost to removing spatially patterned structures. As such, debris of the triangular and striped phases remain, forming boundaries between regions of the majority liquid. The residual striped phase forms three-way connections, partitioning the system into a series of coarsening bubbles. However, the PFC atoms are also dynamically conserved by this infinitesimal energy barrier, which eventually halts the coarsening dynamics.

If we consider that experimentally foams must be prepared by processes more involved than simply quenching a mixture, it seems reasonable to attempt to prepare a foamlike initial condition via some sort of process applied to our system, before we stop and allow the system to evolve on its own. For liquid foams, something such as bubbling and drainage may be used. However, we will consider the simpler process of producing a foam via the expansion or internal production of gas. This method is used in the production of metal foams (and is the responsible for the foam structure of bread). As such, let us consider what happens if material is added to the bubbles over time. We do this by changing the average density of the system to more and more favor the majority phase (reducing ϕ_0) over time. This can provide enough energy to destabilize the PFC atoms while still retaining the stripelike cell walls, which will still remain stable for a longer period as they can move perpendicular to their length to create large bubbles of one of the liquids. The process of reducing the average density strongly influences the immediate coarsening behavior, and so we attempt to inflate the foam as much and as quickly as possible without causing the cell walls to break, after which we stop and allow the foam to coarsen. It is after this time that we begin to make measurements.

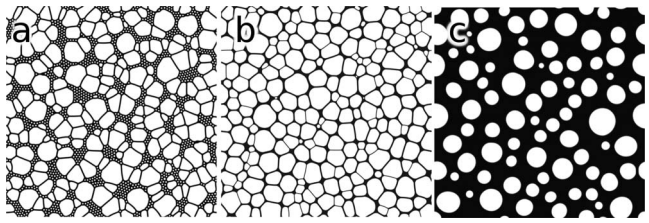

FIG. 2. (a) Final state obtained from Eq. (3) with $\alpha=16$ and $\phi_0=-0.41$ after coarsening. Residual atoms coexist with large foam cell regions. (b) Simulation using the modified PFC equation for $\alpha=20$, quenched with $\phi_0=0.4$ initially, and then drained to $\phi_0=-0.6$. The result is a dry foam structure with no residual atoms. (c) Simulation of the modified PFC equation for $\alpha=20$ and $\phi_0=0.25$, allowed to coarsen without draining. The result is a wet foam structure with circular bubbles.

The end result is a foamlike state [Fig. 2(a)], which coarsens to a stationary point at which there are no more free adjustments that can be made to approach the equilibrium state. Thus, even a small perturbative addition of wavelength selection is sufficient to stabilize a foamlike structure.

Although this behavior is interesting from the point of view of understanding the properties of the phase field crystal model, it does not behave like a physical foam. The arrested coarsening and inability to get rid of residual atoms prevent this from being used as a model for studying coarsening foams. We now alter the free energy so as to destabilize the residual atoms while retaining the overall cellular structure so that we may recover physical foam dynamics.

In effect what we wish to do is to weaken the wavelength selection while encouraging $k=0$ structures. A stripe has one $k=0$ direction and one direction with the selected wavelength, whereas an atom has two directions with the selected wavelength. If the selected wavelength sits at a local energy minimum, but the global minimum is at $k=0$, then this should help remove residual atoms in favor of bubble interfaces.

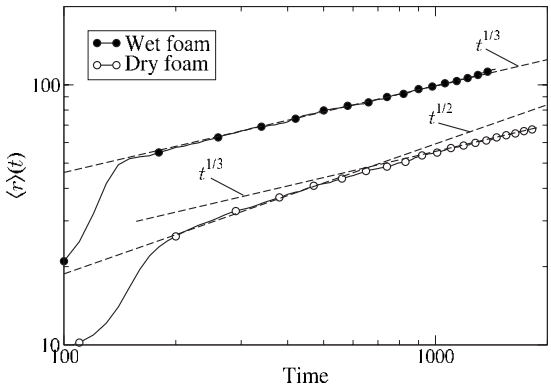

FIG. 3. Coarsening behavior of wet and dry foams in the modified PFC equation with $\alpha=20$, compared with the corresponding theoretical coarsening laws.

The PFC wavelength selection operator $(\nabla^2+1)^2$ corresponds in k space to $E(k)=(1-k^2)^2$. We modify this by introducing two parameters k_0 and b

$$E_{mod}(k) = (k/k_0)^2[1-(k/k_0)^2]^2 - b(k/k_0)^2 \tag{4}$$

and then choose k_0 so as to retain minima at $k=\pm 1$: $k_0 = [3/(2+\sqrt{1+3b})]^{1/2}$. The modified form of the free energy in real space becomes

$$F_{mod} = \int_V \frac{1}{2}\phi\left[-\frac{1}{k_0^2}\nabla^2\left(\frac{1}{k_0^2}\nabla^2+1\right)^2 + \frac{b}{k_0^2}\nabla^2\right]\phi + \alpha\left(-\frac{1}{2}\phi^2+\frac{1}{4}\phi^4\right)dV. \tag{5}$$

We can then vary b to control the relative depths of the minima at $k=\pm 1$. The most extreme effect is achieved at $b=-1/3$, at which the minima at $k=\pm 1$ disappear. We use this value of b throughout the rest of this Rapid Communication. Figures 2(b) and 2(c) show results from the modified PFC equation.

IV. RESULTS

We measured the coarsening dynamics and statistics of the eventual scaling state of the modified PFC equation in order to compare with physical foams. Coarsening behavior can be quantified using the average bubble radius $\langle r\rangle(t)$. We may easily count the total number of bubbles and so determine the average bubble area as $\langle A\rangle(t)=A_{total}/N(t)$. If we assume that deviations from circular geometry are small, then we may approximate $\langle r\rangle(t)\approx\sqrt{\langle A\rangle(t)}$.

For a wet foam, we expect the bubble growth to proceed as diffusive grain growth so that $\langle r\rangle(t)\propto t^{1/3}$. As an example, we simulate a 1024×1024 system with $\alpha=20$ and quench into an average density $\phi_0=0.25$. We observe a scaling $\langle r\rangle \propto t^{0.34}$ (Fig. 3, filled circles), consistent with the predicted growth law.

For a dry foam in two dimensions, von Neumann's law [9] predicts that the growth rate of the bubble area is proportional to $\kappa(n-6)$, where κ is an effective diffusivity and n is the coordination number of the bubble. This implies that the average bubble radius should scale as $\langle r\rangle(t)\propto t^{1/2}$. To measure the coarsening of a dry foam, we quench from an average density $\phi_0=0.3$ and drain slowly to a density of $\phi_0=-0.4$. We start measuring the coarsening dynamics after we have stopped draining. However, our reference point for $t=0$ is still the point of the quench. At early times we observe a scaling $\langle r\rangle\propto t^{0.47}$, which is consistent with von Neumann's law. At late times, we find that the exponent shifts toward 1/3, indicating a transition to wet foam behavior (Fig. 3).

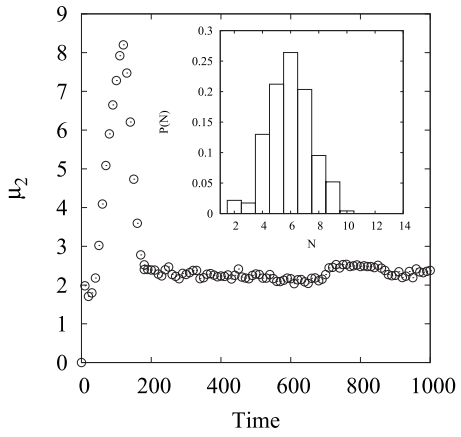

FIG. 4. Evolution of the second moment of the bubble coordination number in a dry foam realized by the modified PFC equation. The bubble distribution broadens during the transition to power-law coarsening, after which it reduces to a steady value of 2.31 ± 0.01. The inset shows a particular distribution at $t=1800$.

As two-dimensional (2D) froths coarsen, they are expected to reach a self-similar scaling state in which the normalized moments of the distribution of areas and of coordination number are expected to become time independent. The second moment of the coordination number distribution has been used as a probe of this scaling state. Glazier and Weaire [10] predict that the coordination number distribution should eventually reach a universal limiting scaling state with a second moment $\mu_2=1.4$, with a strongly nonmonotonic transient behavior.

We measure the coordination number distribution of the dry foam by a watershed algorithm [11]. We superimpose a grid over the system and fill each bubble with a unique integer. We then allow these integers to propagate to neighboring unoccupied cells and then find the total number of different integers that a given bubble comes into contact with. We observe a similar time dependence of the second moment of our distribution, but the measured limiting value $\mu_2=2.31\pm0.01$ is significantly different from 1.4 (see Fig. 4). In other models and simulations of coarsening 2D foams, the observed limiting value of μ_2 has been variously reported as 1.9 [12], 1.7 [13], and 1.5 [14], and experiments have measured from 1.4 [15] in soap froths to values as small as 0.14 and 0.22 in magnetic froths [16].

We conclude that the either second moment is not a universal quantity or that there are strong transients that make any universal scaling regime difficult to observe in practice. We note that our foam is not completely dry and that the absence of a drainage mechanism implies that the foams becomes wetter the more they coarsen. Whether real foams

undergo a corresponding change in regime is not clear.

We have found that in the limit of large undercooling, the phase field crystal equation produces topologically stabilized foams. These foams are a consequence of the residual wavelength selection, which acts as a singular perturbation that prevents the destruction of cell walls and forces the coarsening to take place via topological rearrangements. The fact that this behavior emerges from a minimal model such as the phase field crystal equation suggests a general mechanism by which foams may occur in natural systems.

The ingredients of the phase field crystal equation are a driving force toward certain equilibrium densities, some sort of spatial relaxation (diffusion, viscosity, etc.), and some competing source of wavelength selection. Such a system, in the limit where the wavelength selection is weak compared to the other forces, would likely give rise to a foam. This mathematical structure can be seen in models of magnetic froths [16], type-I superconductors [17], and in models of polygonal cells found in melting snow [18].

However, the foams produced in this limit of the PFC equation have unphysical properties. The wavelength selection also preserves atoms: bubbles whose diameter is comparable to the width of the cell walls. This can be ameliorated by modifying the PFC free energy to penalize atoms while encouraging stripes. As a result, the coarsening dynamics of real foams are recovered although the distribution of bubbles in the resultant scaling state appears to be somewhat different.

If these differences are understood, the modified PFC equation may be a useful tool in modeling foams, as it is simpler than other existing methods, such as Q-Potts models [19] and minimal surface evolution [20], and is fairly easy to simulate, having only one field and a spatial structure that is easily treated with spectral methods.

ACKNOWLEDGMENTS

We are grateful to B. Athreya for discussions about the stability of the PFC equation. N. Guttenberg was supported by the University of Illinois, and J.D. acknowledges the support of the (U.S.) Department of Energy, under Contract No. 4000076535.

[1] K. R. Elder and M. Grant, Phys. Rev. E **70**, 051605 (2004).
[2] K. R. Elder, N. Provatas, J. Berry, P. Stefanovic, and M. Grant, Phys. Rev. B **75**, 064107 (2007).
[3] N. Provatas, J. Dantzig, B. Athreya, P. Chan, P. Stefanovic, N. Goldenfeld, and K. Elder, JOM **59**, 83 (2007).
[4] J. Mellenthin, A. Karma, and M. Plapp, Phys. Rev. B **78**, 184110 (2008).
[5] P. Y. Chan, N. Goldenfeld, and J. Dantzig, Phys. Rev. E **79**, 035701(R) (2009).
[6] P. Y. Chan and N. Goldenfeld, Phys. Rev. E **80**, 065105(R) (2009).
[7] N. Goldenfeld, B. P. Athreya, and J. A. Dantzig, Phys. Rev. E **72**, 020601(R) (2005).
[8] S. A. Brazovskii, Zh. Eksp. Teor. Fiz. **68**, 175 (1975).
[9] J. Von Neumann (Am. Soc. Test. Mater., Cleveland, OH, 1952), p. 108.
[10] J. Glazier and D. Weaire, J. Phys.: Condens. Matter **4**, 1867 (1992).
[11] F. Meyer, *8me Congrès de Reconnaissance des Formes et Intelligence Artificielle* (AFCET, Paris, 1991), Vol. 2, pp. 847–857.
[12] M. Marder, Phys. Rev. A **36**, 438 (1987).
[13] H. Flyvbjerg, Phys. Rev. E **47**, 4037 (1993).
[14] J. Glazier, M. Anderson, and G. Grest, Philos. Mag. B **62**, 615 (1990).
[15] J. Stavans and J. A. Glazier, Phys. Rev. Lett. **62**, 1318 (1989).
[16] F. Elias, C. Flament, J. C. Bacri, O. Cardoso, and F. Graner, Phys. Rev. E **56**, 3310 (1997).
[17] R. Prozorov, A. Fidler, J. Hoberg, and P. Canfield, Nat. Phys. **4**, 327 (2008).
[18] T. Tiedje, K. Mitchell, B. Lau, A. Ballestad, and E. Nodwell, J. Geophys. Res. **111**, F02015 (2006).
[19] Y. Jiang and J. Glazier, Philos. Mag. Lett. **74**, 119 (1996).
[20] R. Phelan, D. Weaire, and K. Brakke, Exp. Math. **4**, 181 (1995).